Fermilab

TM-1044
1600.000
February 1981

THE FERMILAB TEVATRON

Lee C. Teng
Fermi National Accelerator Laboratory
P.O. Box 500, Batavia, Illinois 60510

The Fermilab Tevatron Project[1] consists of three phases. These are:

Phase 0 (Saver)	Superconducting magnet ring	A
	Minimal refrigeration and rf (for slow acceleration of a beam to ~1 TeV)	A
Phase I (TEV 1)	Additional refrigeration and rf (for fast pulsing up to ~2 min^{-1})	B
	$\bar{p}p$ colliding beams ($\bar{p}$ source, accelerator and enclosure modifications)	C
Phase II (TEV 2)	Beam extraction and switchyard modifications	B
	Experimental areas and beams modifications and additions	B

The reason for the particular grouping into phases is historical, but the physics capability of the facility is staged as shown by the priority assignment given in the last column, namely

Priority A Resolve all technological problems of a superconducting magnet synchrotron and demonstrate capability by accelerating some beam to ~1 TeV.

Priority B Provide capability and facility for doing fixed target physics at beam energies up to ~1 TeV and intensities up to ~10^{12} protons/sec.

Priority C Provide capability and facility for doing $\bar{p}p$ colliding beams physics at energies up to ~1 TeV + 1 TeV and luminosities up to ~$10^{30} cm^{-2} sec^{-1}$ (The detector will be funded separately.)

In round numbers each of the three phases is budgeted at ~$50 million. Saver has been authorized and funded and is scheduled for completion by 1982. TEV 1 has also been authorized and received initial funding in 1981. Construction will be started soon. TEV 2 is expected to be authorized for initial funding in 1982. Different parts of the project have various scheduled completion dates, but all parts should be completed by 1984. After commissioning the total project will

provide:

1. the first superconducting magnet synchrotron
2. the first 1 TeV beam
3. the first 2 TeV colliding beams,

and will represent a tour-de-force accomplishment both technologically and scientifically. It will enable us to produce and examine more closely events such as the Centauros which were generated, so far, only by cosmic ray particles at energies of $\sim 10^{15}$ eV. In the following we will give a description and status report of the Tevatron Project by priority groups.

Priority A - Saver Ring

First, some general statements about superconducting magnets. Compared to conventional magnets, superconducting magnets have the following features. (Numbers give ratios of superconducting values to conventional values. For superconducting magnets we assume NbTi conductors operating at 4.5 K, but because of large variations in cable and magnet designs all these numbers have large ranges.)

1. High current density, hence high field.

	d.c.	pulsed
Current density	70	40
Dipole field	2 to 3	
Quadrupole gradient	3 to 4	

For conventional magnets when operated in triangular pulses the average power is $\sim\frac{1}{3}$ of the peak power, hence the maximum practical current density is $\sim\sqrt{3}$ that of d.c. operation.

2. Low power consumption, low power supply cost.

	d.c.	pulsed (1 min^{-1})
Power consumption	$\frac{1}{100}$	$\frac{1}{10}$
Power supply cost	$\frac{1}{100}$	$\frac{1}{3}$

For superconducting magnets the a.c. heating is rather large during pulsed operation. At a pulse rate of 1 pulse/min the required refrigeration

power is ~3 times that of d.c. operation.

3. Large field errors

	d.c.	pulsed
Systematic errors	8	30
Random errors	4	4

The comparisons are made at sufficiently high fields so that the remanent field and the persistent current effects are negligible. In superconducting magnets the field shape is determined by the placement of conductors which cannot be done with the same accuracy as the shaping of steel poles of conventional magnets. Furthermore, when pulsing superconducting magnets excursions in the very large magnetic forces deform the coils and cause sizeable variations in systematic field errors.

From this we see that the principal advantage of superconducting magnet is the ~100-fold savings in power consumption for d.c. applications. This is most crucial since it is likely that in the future all ring accelerators must be capable of being operated d.c. for colliding beams. The factor of 2 to 4 in peak field is nice but certainly not critical. For pulsed application as in a synchrotron the advantage of superconducting magnets is not very prominent due to both the relatively large a.c. heating and the large systematic field errors. Systematic errors can be corrected but correction requires effort and equipment. A.C. heating limits the pulse rate through the available refrigeration power. Also the quench current of the superconductor deteriorates substantially at pulse rates much above 2 pulse/min. The conventional magnet Fermilab main synchrotron can operate at pulse rates up to 10 pulse/min limited only by the power supply capabilities.

Another difficulty in the use of superconducting magnets for accelerator is quenching by stray radiation. Because of the very low heat capacity at liquid helium temperature the superconductor will quench if heated by ~$\frac{1}{2}$ mJ/g (~5×10^7 GeV/cm^3) in a time too short for the cooling by the refrigerant to be

effective, say, <1 msec. The shower developed by one high energy proton will deposit some 5×10^{-3} GeV/cm^3. Therefore it takes a stray beam of only 10^{10} proton/cm^2 striking the superconducting coil in <1 msec to cause the magnet to quench. Thus, while superconducting magnets are crucial for some applications their use is by no means simple.

The Tevatron magnets have warm iron-yokes. This design has two very important advantages.

1. Since only the coil assembly with a small fraction of the total magnet mass is cooled, the refrigeration capacity required is greatly reduced and the cool-down time is cut from days to hours.

2. The iron yoke is situated in regions of lower magnetic field away from the coil and is never saturated, thereby avoiding a large systematic field error introduced by saturation of the iron yoke during pulsing.

These advantages are gained, however, at a cost. During cool-down the cold coil assembly shrinks away from the warm yoke making the anchoring of the coil assembly difficult. The anchors provided in the original design of the Tevatron dipole were inadequate and allowed the coil assembly to rotate axially by a small amount at each cooldown. This difficulty caused a temporary stoppage of production last summer. The support was beefed up by using spring-loaded bolts (see Fig. 1) as anchors which can take up the differential contraction on cooldown. The dipole production was resumed in August.

Training is no longer a problem. All production magnets train in fewer than 3 quenches with many attaining full field on the first pulse. Each production dipole undergoes a very rigid testing and measurement program. In addition to a number of mechanical, vacuum and electric breakdown tolerances we specify acceptable values of

1. minimum quench current
2. maximum a.c. heating
3. maximum quench current when the quench-protection heater is on

4. maximum axial rotation during several cooldowns

5. maximum field errors, etc.

Over 95% of the production dipoles pass the test.

The first production quadrupole and the first set of correction coils (inside the spoolpiece) have just been successfully tested. Systems operation experiences are being gained on one test-string of 16 dipoles and 4 quadrupoles and another string of 21 dipoles which is now being used to deflect the 400 GeV beam into the meson experimental area. Some 30 dipoles have already been installed in the tunnel underneath the main ring (Fig. 2). A comparison between the projected and the actual production of dipoles is shown in Fig. 3. The present rate of production is ~4 per week. We intend to increase the production rate to 10 per week by going to full three-shift operation. The overall production and installation schedule of the Saver ring is shown in Fig. 4.

Priority B - Fixed-Target Facility

To make the Saver ring useful for doing fixed-target physics the following additions and modifications are necessary.

1. Addition of sufficient refrigeration and rf acceleration capabilities to enable pulsing the Saver ring at the highest rate allowed by the superconducting magnets. At present, this limit is ~2 pulse/min, corresponding to a ramp rate up and down of ~75 GeV/sec and a flat-top of ~5 sec.

2. Addition of a 1 TeV slow extraction system and modification of the switchyard for splitting and transporting 1 TeV beams.

3. Modifications of the experimental areas, and modifications and additions of experimental beams.

Items 1. and 2. are straightforward and need no further elucidation. The almost fixed frequency rf system for the Tevatron is simpler than that for the main ring. The same half-integer resonant beam extraction system as that of the main ring will be used. With the more stable and ripple-free superconducting magnet ring a smooth spill of several seconds should not be difficult to achieve. The major

difficulty in the design of the system is to provide adequate radiation shielding where stray or scattered beam may strike a superconducting magnet causing it to quench. The maximum pulse rate of 2 min^{-1} is some factor 3 lower than that of of the main ring. This implies a corresponding reduction in the average beam intensity unless one can inject more than one main ring pulse into the Saver ring. More experience and detailed study are necessary to determine whether this is indeed feasible.

Item 3. is shown diagramatically in Fig. 5. Major new beams added are:

a. Broad-band electron/photon beam

This is a straight single-stage momentum analyzed beam ~300 m in length. Dispersion is introduced at the midpoint of a 3-dipole local orbit displacement where the momentum slit and the neutral dump are located. The yield is good because of a very large momentum acceptance of ±15% and a large solid angle of 4 μsr. Even at 600 GeV/c the yield is close to 10^{-5} electron per interacting 1-TeV proton. The beam can transport electrons up to 800 GeV/c and because the net deflection is zero, can be made into a neutral beam by simply removing the neutral dump.

b. Polarized proton/antiproton beam

Polarized protons (antiprotons) are obtained from the decays of Λ's ($\bar{\Lambda}$'s). This is a tertiary beam similar to the μ beam, but much shorter in length because of the much shorter life time of Λ. Lambdas are produced by 1-TeV protons striking a primary target. After the target the remaining primary protons and charged secondaries are dumped by a sweeping magnet. The Λ's travel straight on and decay to give polarized p's. From the target to the end of the decay channel is only ~40 m. The polarized p's then go through a ~240 m long beam transport in which they are momentum/polarization selected, have their polarization precessed to the desired plane by a series of dipoles (the snake), and are finally focused onto the experimental target. The maximum polarization obtainable is ~45%. For a 10% momentum bite the beam intensity is 10^7 to 10^8 polarized

p's between 70 and 800 GeV/c or $\frac{1}{2}\times 10^6$ to $\frac{1}{2}\times 10^7$ $\bar{p}$'s between 70 and 400 GeV/c with 3×10^{12} 1-TeV p's on target.

c. High energy muon beam

This is a more-or-less standard 10-cell (7 cells for decay channel and 3 cells for muon transport) FODO quadrupole muon channel, but is extremely long, ~1700 m, because of the high energy. The yield of μ^+ is summarized in the following table.

Momentum (GeV/c)	μ^+/p-interacting (10^{-5})	Halo (3m x 3m area)
275	30	7%
550	9.0	4%
750	1.2	8%

The momentum bite is $\frac{\Delta p}{p}$ = 20% FWHM but can be tagged to 2%. The beam spot size is 40 cm(h) x 2 cm(v) FWHM.

In addition to these major new beams the top momenta and intensities of all secondary and tertiary beams will be greatly increased as a result of the factor 2.5 increase in the primary energy from 400 GeV to 1000 GeV. This is especially true for tertiary beams such as the neutrino beam. With various focusing devices the ν flux on a 1 m^2 detector at 1400 m from primary target is $10^5 - 10^7$ GeV^{-1} up to 600 GeV, with 10^{13} 1-TeV protons on target. We expect that this facility will open up a new broad vista of fixed-target physics.

The physics and preliminary engineering design for the facility is complete. Detailed design has started on many of the components in anticipation of initial funding in 1982.

Priority C - Colliding-Beams Facility

The crucial advantage of a superconducting magnet ring is that it can be operated d.c. at the top field to serve as a storage ring for colliding beams of a particle and its antiparticle, p and $\bar{p}$ for the Tevatron. What one needs in addition are:

I. A source of high phase-space density $\bar{p}$, and

II. Some modification of the ring to focus the p and $\bar{p}$ beams to high spatial density at the collision point to enhance the luminosity.

We will discuss these in the following.

I. Antiproton source

Antiprotons produced by a high energy proton beam striking a target have very low phase-space density. Hence only a small number of $\bar{p}$ can be contained in the rather limited phase-space acceptance of the Saver ring. There are two methods presently available to increase the phase-space density or, equivalently, to reduce the phase-space volume occupied by the beam - a process similar to cooling a volume of gas molecules.

1. Electron cooling

Because of the much lower mass electron beams colder (lower random kinetic energy) than the $\bar{p}$ beam can be produced relatively easily. A cold electron beam with the same velocity is made to travel along and mix with the stored $\bar{p}$ beam in a straight section of the storage ring. In the rest frame this is just a 2-component plasma. Equipartition of energy between the 2 components through Coulomb interaction will cool the antiprotons and heat the electrons. For this application the cooling is adequately fast only for $\bar{p}$ energies less than a few hundred MeV (see Appendix 1). At 200 MeV with a rather heroic but still realistic electron beam a cooling time of a few tenths of a second can be obtained.

2. Electronic cooling (Stochastic cooling)

Because the $\bar{p}$ beam is not a continuum but an ensemble of a finite number of individual particles a broad-band electronic feedback system could be used to cool the beam.* A pickup electrode senses the statistical fluctuation

*Liouville theorem applies only to the mathematical phase-space volume, i.e. a continuum.

of the off-center displacement of the centroid of a small sample of $\bar{p}$'s. The signal is amplified and applied to reduce the displacement by a kicker located downstream of the sensor. It is important that the sample remains more-or-less identifiable (not totally mixed with other $\bar{p}$'s) between the sensor and the kicker. It is also important that before returning to the sensor the sample should be mixed (at least partially) with other $\bar{p}$'s in the beam so that with each revolution new statistical fluctuations are presented to and reduced by the feedback electronics. The cooling rate is limited by the bandwidth, the noise, and the output power of the electronics. This scheme is particularly advantageous for longitudinal (momentum) cooling because in this degree of freedom the pickup signal is a frequency which can be easily cleaned up by a filter. For a 4.5 GeV beam of 10^7 $\bar{p}$'s a momentum (longitudinal) cooling time of a few seconds is obtainable (see Appendix 2).

The collecting, cooling and accumulating of the $\bar{p}$ beam is done as follows (see Fig. 6). Protons accelerated to ~100 GeV in the main ring are extracted and made to strike a $\bar{p}$-production target. The $\bar{p}$'s produced at 4.5 GeV are collected in a precooler ring and momentum cooled by electronic cooling. The beam is then decelerated (while momentum cooling continues) to 200 MeV and transferred to an electron cooling ring where it is cooled in all 3 dimensions by electron cooling. As soon as the beam is transferred out of the precooler ring 10 seconds after injection the next main ring pulse begins over again. The cold $\bar{p}$ beams from all the main ring pulses are stacked, stored, and continually cooled in the electron cooling ring. It takes some 10 hours to accumulate 10^{11} $\bar{p}$'s. This precious cold $\bar{p}$ beam is then accelerated in normal sequence to 150 GeV and injected into the Tevatron in a direction opposite to that of protons. A normal 150 GeV proton beam is now also injected into the Tevatron. Finally both beams are accelerated simultaneously to 1 TeV for 1 TeV + 1 TeV colliding $\bar{p}p$ beams.

One complication in the scheme is that when a main ring pulse

of $>2\times10^{13}$ of ~100 GeV protons strike the $\bar{p}$-production target at once, the thermal shock will cause the target to explode. Therefore the main ring beam will have to be extracted in pieces or in a long spill to provide time for either moving the target or removing the heat by a cooling system.

The crucial parameter for the scheme is clearly the $\bar{p}$ accumulating rate. We give here an estimate. The production cross-section is given by

$$\sigma = \left(E \frac{d^3\sigma}{dp^3} \right) \frac{1}{E} p^3 \frac{\Delta p}{p} \Delta\Omega$$

where

$E \frac{d^3\sigma}{dp^3}$ = invariant cross-section for $\bar{p}$-inclusive production

$\cong$ 0.8 mb/GeV^2 (More precise measurement is planned.)

p (momentum) $\cong$ E (total energy) $\cong$ 5.4 GeV (for 4.5 GeV kinetic energy)

$\frac{\Delta p}{p}$ = momentum bite accepted = 1%

$\Delta\Omega$ = solid angle accepted = 1.5 msr.

This gives

$$\sigma = 3.5\times10^{-4} \text{ mb.}$$

The number of $\bar{p}$ produced per p on target is, therefore

$$\frac{N_{\bar{p}}}{N_p} = \frac{\sigma}{\sigma_{abs}} \varepsilon_T = \frac{3.5\times10^{-4} \text{ mb}}{33 \text{ mb}} \times 10\% = 10^{-6}$$

where σ_{abs} = 33 mb is the total absorption cross-section of the proton and ε_T = 10% is the targetting efficiency. At the present main ring operating intensity of 2.6×10^{13} p every 10 sec, this gives a $\bar{p}$ accumulating rate of ~10^{10} per hour.

II. Tevatron modification and luminosity

Quadrupoles must be added to either side of the collision point in a long straight section to focus the beams to narrow waists at the collision point

to enhance luminosity. By adding 4 quadrupoles—2 on each side located more than 7.5 m away from the collision point—one can obtain a $\bar{p}$ beam spot radius of 0.12 mm or a cross-sectional area of 0.047 mm^2. With 10^{11} $\bar{p}$'s circulating at a revolution frequency of 48 kHz the flux is $\frac{10^{11} \times 48 \text{ kHz}}{0.00047 \text{ cm}^2} \cong 10^{19} \text{ cm}^{-2}\text{sec}^{-1}$. The $\bar{p}$'s strike a target formed by a bunch of 10^{11} protons. This gives a luminosity of

$$L = (10^{19} \text{ cm}^{-2}\text{sec}^{-1}) \times 10^{11} = 10^{30} \text{ cm}^{-2}\text{sec}^{-1}.$$

The 10^{11} $\bar{p}$'s can be in several bunches as long as the p beam is so tailored that when a $\bar{p}$ bunch arrives at the collision point a bunch of 10^{11} p is there to provide a target.

As mentioned earlier TEV I has been authorized and initial funding was provided in FY 81. But the detailed apportionment of funds for the various parts of TEV I will depend, of course, on their priority assignments. It is also obvious that the Colliding Beams Facility entails the development of a number of components requiring new and frontier technology. Efforts are now being spent to examine the many facets of the design to gain experience and assurance.

Appendix 1 Electron Cooling Rate[2]

This is a standard problem for a 2-component plasma. We give here a sketch of the derivation for a simplified case. The velocity dependent "friction" force on a test charge (in this case the $\bar{p}$) moving in a spatially uniform electron distribution $f(\vec{v})$ is given by

$$\vec{F}(\vec{v}) = -(4\pi e^4 \frac{n_e^*}{m_e} \ell n\Lambda)\nabla_v \phi$$

with the "potential" ϕ given by the Poisson-like equation in the velocity space

$$\nabla_v^2 \phi = -4\pi f(\vec{v})$$

where

e, m_e = charge, mass of electron

n_e^* = spatial density of electron distribution (* denotes value in rest-frame)

$\ell n\Lambda = \ell n\ (12\pi\ n_e^*\ \lambda_D^3)$ = Coulomb logarithm

$$\lambda_D = \left(\frac{1}{4\pi r_e} \frac{\bar{\beta}_e^2}{n_e^*}\right)^{1/2} = \text{Debye screening length}$$

$$r_e = \frac{e^2}{m_e c^2} = \text{classical electron radius}$$

$\bar{\beta}_e$ = rms value of the random part of $\frac{v}{c}$ in the rest frame of the electron distribution (related to the "temperature").

A swarm of $\bar{p}$'s will be cooled ("attracted" to the "velocity center" of the electron distribution) at the rate

$$\frac{1}{\tau^*} = \frac{1}{m} \nabla_v \cdot \vec{F} = \frac{1}{m} (4\pi e^4 \frac{n_e^*}{m_e} \ell n\Lambda)(-\nabla_v^2 \phi)$$

$$= (4\pi)^2 \frac{e^4}{m m_e} n_e^*\ \ell n\Lambda f(\vec{v})$$

where m and $\vec{v}$ are the mass and the velocity of the $\bar{p}$. Assuming Maxwellian electron distribution and $v \ll v_e$ (Because of the much larger $\bar{p}$ mass this is generally valid even though the $\bar{p}$ beam is hotter - higher random energy.), and transforming to the lab-frame we get

$$\frac{1}{\tau} = \sqrt{32\pi}\, r_e r_p \ell n \Lambda \left(\frac{1}{\beta\gamma^2} \frac{j_e/e}{\bar{\beta}_{ex}\bar{\beta}_{ey}\bar{\beta}_{ez}} \right) \eta$$

where

$r_p = \frac{e^2}{mc^2}$ = classical $\bar{p}$ radius

$\beta\gamma^2$ = relativistic kinematic factor of the $\bar{p}$ beam (identical for the e beam)

j_e/e = number current density of the electron beam

$\bar{\beta}_{ex}, \bar{\beta}_{ey}, \bar{\beta}_{ez}$ = standard deviations (rms) of the (Maxwellian) electron distribution in the rest-frame and in the 3 degrees of freedom indicated by the subscripts.

η = duty factor = fractional part of the $\bar{p}$ orbit overlapping with electron beam for cooling.

This shows that the cooling rate is higher for:

1. higher electron current density j_e
2. colder electron beam (smaller $\bar{\beta}_e$)
3. lower $\bar{p}$ beam energy (smaller $\beta\gamma^2$).

The realistically attainable cooling rate is unfortunately rather low for this application. Even for 200 MeV $\bar{p}$'s cooled over η = 5% of the circumference by a rather heroic electron beam of 1 A/cm^2 and as cold as $\bar{\beta}_{ex} = \bar{\beta}_{ey} = \bar{\beta}_{ez} = 10^{-3}$ (rms energy in each dimension $\cong \frac{1}{4}$ eV) we get

$$\frac{1}{\tau} = 2.1 \text{ sec}^{-1}.$$

Thus, for $\bar{p}$ accumulation electron cooling is too slow at GeV energies.

Appendix 2 Electronic cooling (stochastic cooling) rate[3]

We give here without derivation the formula for the cooling rate and discuss its features and implications. The formula is

$$\frac{1}{\tau} = \frac{W}{2N}\left[2g - g^2\left(\frac{1}{n}\sum_{k=1}^{n}\frac{f_o}{w_k} + \eta\right)\right]$$

where

W = bandwidth of the feedback system

N = number of particles in beam

g = "gain" = fractional correction in one pass ($\Delta x = -gx$)

$\eta = \frac{\text{noise power}}{\text{signal power}}$

f_o = revolution frequency

$n = \frac{2W}{f_o}$ = number of Schottky bands

w_k = width of k^{th} Schottky band.

We observe the following.

1. The factor $\frac{W}{N}$ is obvious. If $W = N$ one should be able to sample all the particles individually in 1 second.

2. For given $\frac{W}{N}$ the cooling rate has a maximum of

$$\left(\frac{1}{\tau}\right)_{max} = \frac{W}{2N}\left(\frac{1}{n}\sum_{k}\frac{f_o}{w_k} + \eta\right)^{-1}$$

at

$$g = \left(\frac{1}{n}\sum_{k}\frac{f_o}{w_k} + \eta\right)^{-1}.$$

3. For perfect mixing each Schottky band has a width equal to the revolution frequency, namely $w_k = f_o$ and

$$\frac{1}{n}\sum_{k}\frac{f_o}{w_k} = \frac{1}{n}\sum_{k=1}^{n} 1 = \frac{n}{n} = 1.$$

Thus, with zero noise ($\eta = 0$) and perfect mixing one should make $g = 1$ and obtain

an optimum

$$\left(\frac{1}{\tau}\right)_{max} = \frac{W}{2N} .$$

4. Noise and poor mixing limit the useable gain. Generally for longitudinal cooling we have

$$\frac{1}{n} \sum_k \frac{f_o}{w_k} + \eta \cong 10^3 \quad \text{(order of magnitude)}.$$

Hence the optimal "gain" is only $g = 10^{-3}$ and with a bandwidth of 2 GHz for a beam of 10^7 particles we get

$$\frac{1}{\tau} \cong \frac{2\times10^9 \text{ sec}^{-1}}{2\times10^7} \times 10^{-3} = \frac{1}{10 \text{ sec}} .$$

Again the cooling is slow, but fortunately at such a low "gain" the ampliflier power required is attainable even at $\bar{p}$ energies of several GeV. The electronic cooling scheme is particularly advantageous for longitudinal cooling because in this dimension the pickup signal is a frequency which can be easily cleaned up by a filter to give a much smaller η.

References

1. The details of the Tevatron Project are contained in three Fermilab Design Reports:

"A Report on the Design of the Fermi National Accelerator Laboratory Superconducting Accelerator", May 1979

"Design Report - Tevatron Phase 1 Project", February 1980

"Design Report - Tevatron Phase 2 Project", May 1980

2. Electron cooling was proposed by G.I. Budker and first demonstrated at the Institute of Nuclear Physics, Novosibirsk, in 1974. For theoretical treatments see

T. Ogino and A.G. Ruggiero, "Theory of Electron Cooling with Magnetic Field and Space Charge", Particle Accelerators, Vol. 10, No. 3-4, pp. 197-205 (1980) and the many references given in the article.

For the Fermilab effort see

"Fermilab Electron Cooling Experiment - Design Report", August 1978.

3. Electronic cooling (stochastic cooling) was first proposed by S. van der Meer and first demonstrated on the CERN-ISR in 1973. The most comprehensive discussion of the subject is given in

D. Möhl, G. Petrucci, L. Thorndahl and S. van der Meer, "Physics and Technique of Stochastic Cooling", Physics Reports, Vol. 58C, No. 2, pp. 73-119 (1980)

Figure 1. Saver dipoles showing the spring loaded anchor bolts (18 per dipole) which support the coil assembly inside the yoke.

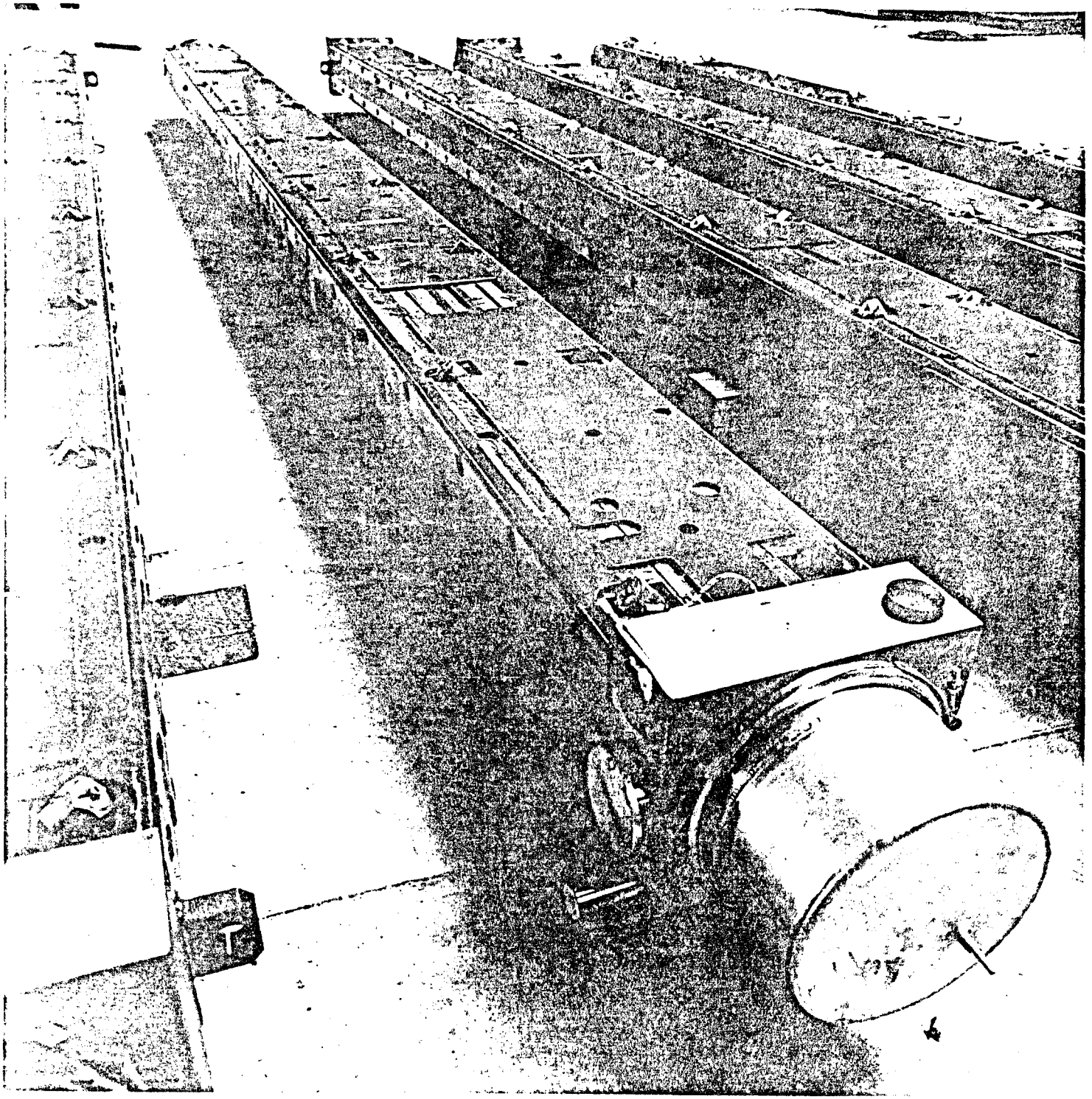

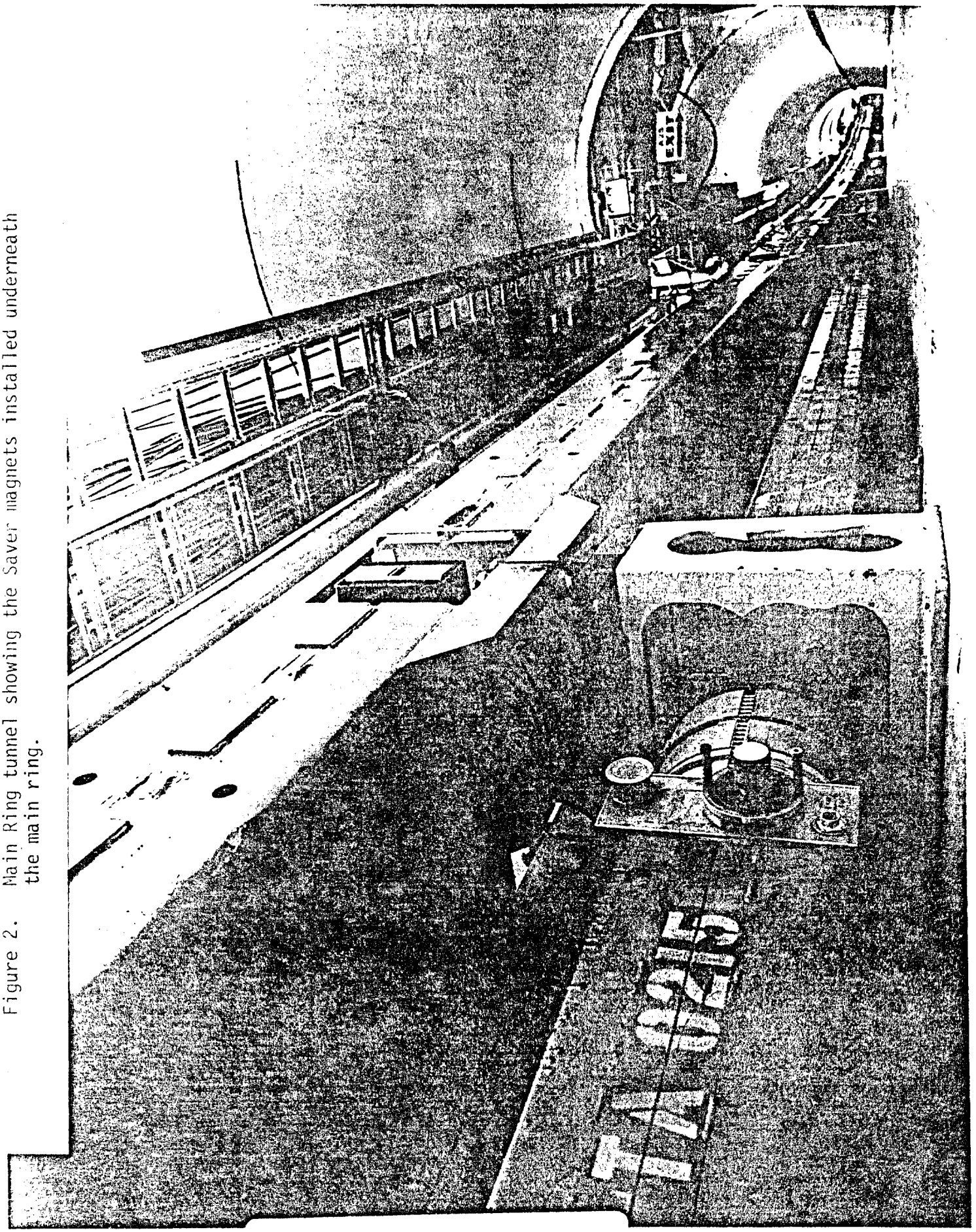

A-Sector Tunnel Installation

Figure 2. Main Ring tunnel showing the Saver magnets installed underneath the main ring.

Figure 3. Comparison between the projected and the actual production schedules of Saver dipoles.

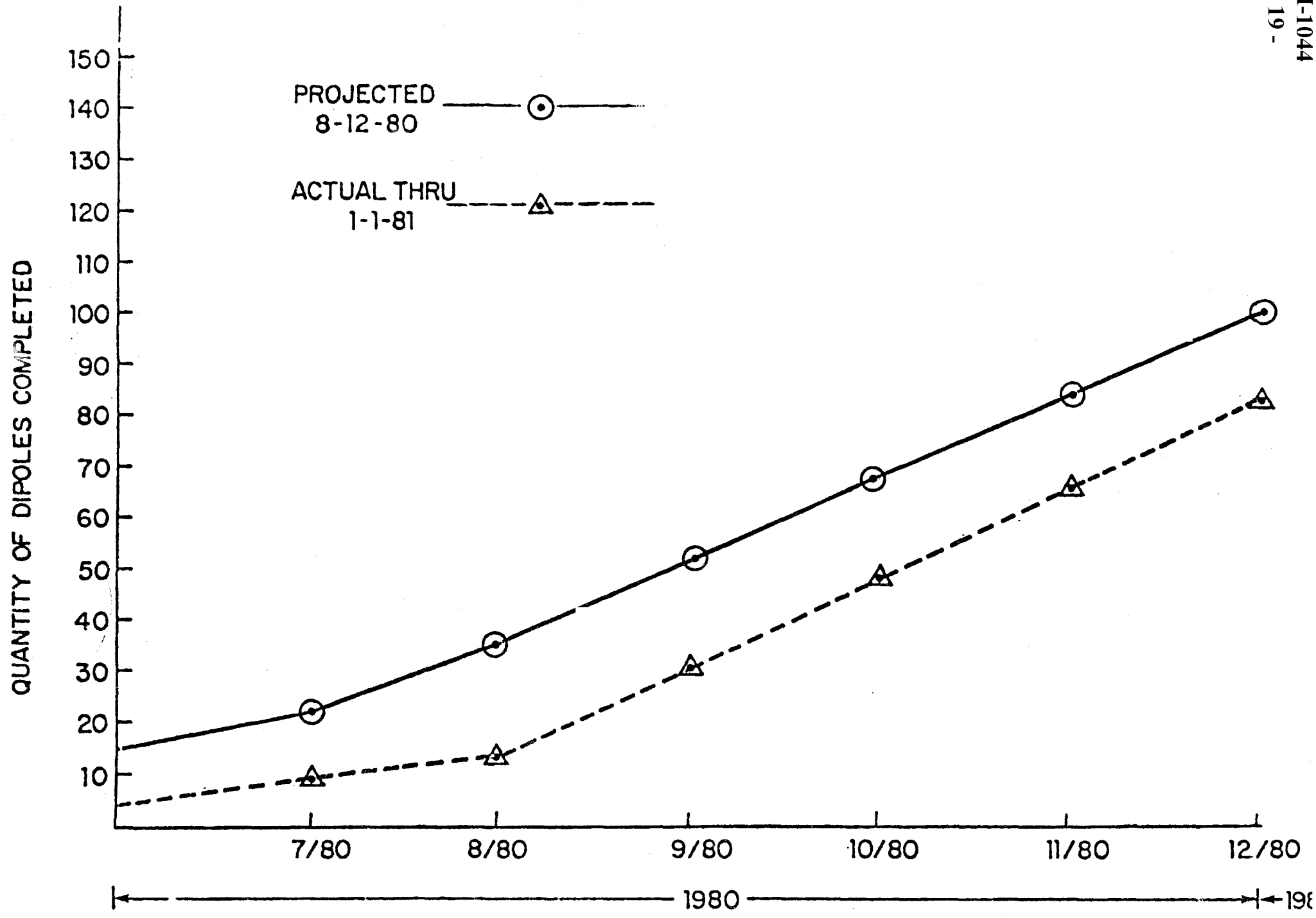

Figure 4. Overall production and installation schedule of the Saver ring.

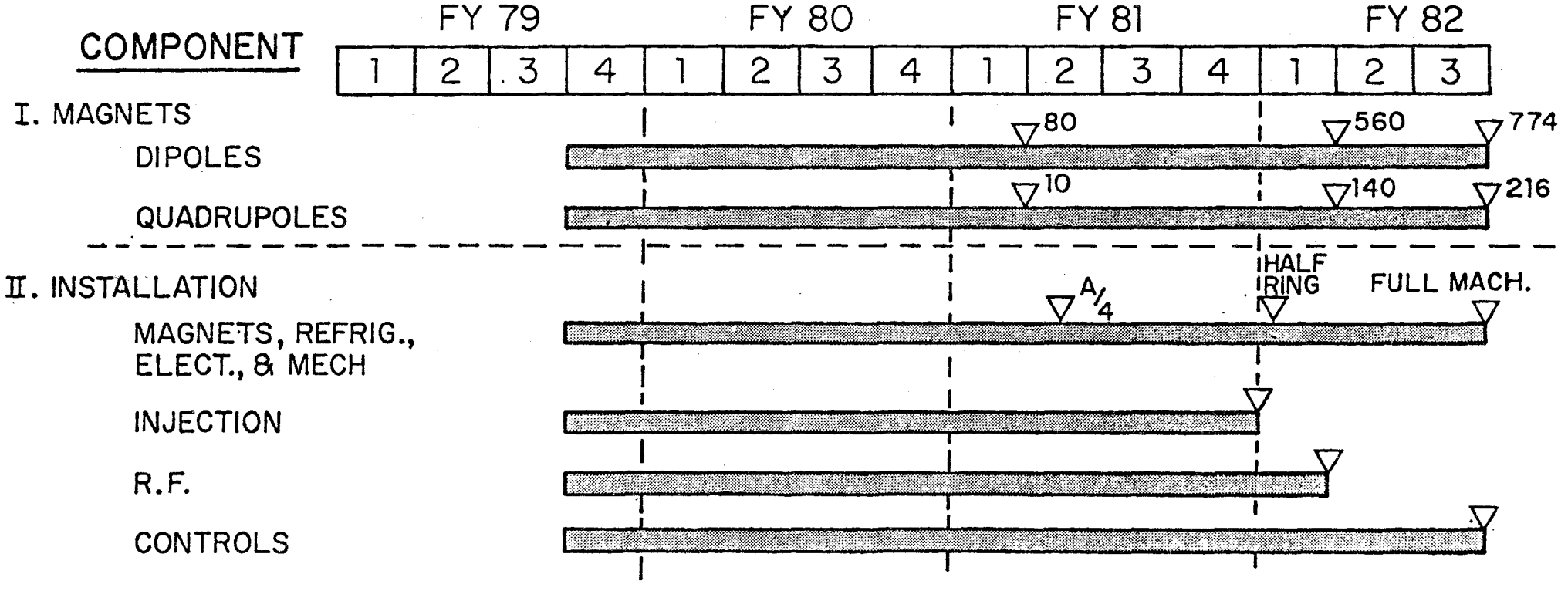

Figure 6. Layout of TEV 1 antiproton source showing the p-production target, the precooler ring and the electron cooling ring.

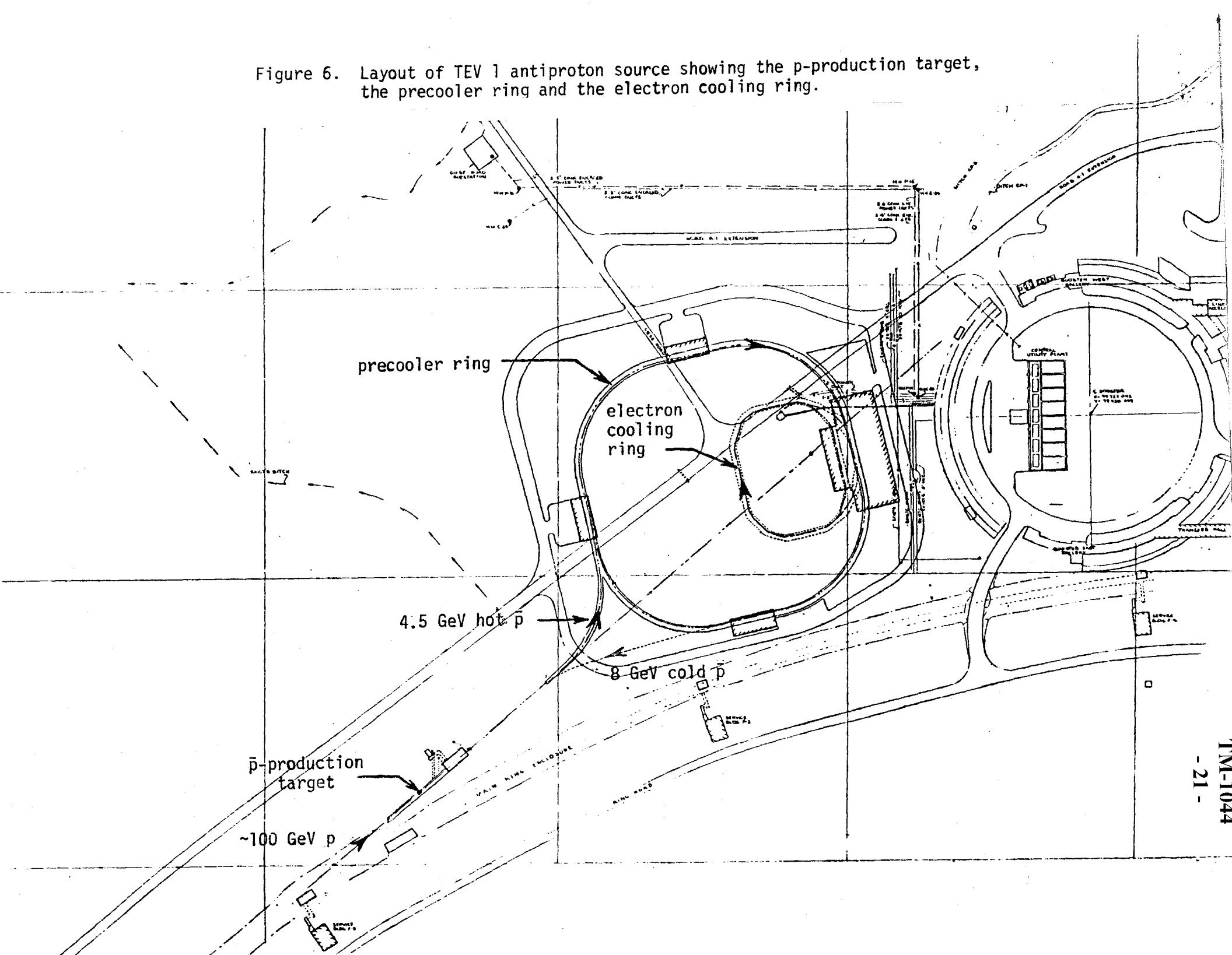

Figure 5. Schematic of TEV 2 construction